

The Effect of Engine Wear on Performance in the NSTAR 8000 Hour Ion Engine Endurance Test*

J. E. Polk, J.R. Anderson, J. R. Brophy, V. K. Rawlin, M. J. Patterson, J. Sovey

Abstract

One of the objectives of an ongoing wear test of the NSTAR ion thruster is to gain an understanding of how engine wear or aging affects performance. In the 6500 hours of operation achieved to-date, performance changes at the full power operating point have been negligible. Periodic throttling tests over the design power range of the thruster also show minimal changes at all but the lowest power level. The observed decreases in total efficiency are due to increased ion production costs. A model of discharge chamber operation was used to identify wear processes that could potentially affect thruster performance. Two phenomena observed in the wear test appear to be particularly important. Enlargement of accelerator grid apertures by sputter erosion, which leads to increased neutral losses, and an increase in the ion current collected by the screen grid have occurred and contribute to the observed performance changes. The model demonstrates qualitatively that the performance impacts of these wear processes are greater at low propellant flow rates, explaining the greater losses seen at low power levels.

Introduction

Xenon ion propulsion is finally entering an age of application in NASA's planetary program. A xenon ion primary propulsion system is one of the key technologies to be demonstrated on Deep Space 1, the

*Copyright 1997 by the American Institute of Aeronautics and Astronautics, Inc. The U.S. (government has a royalty-free license to exercise all rights under the copyright claimed herein for governmental purposes. All other rights are reserved by the copyright owner.

first of the New Millennium missions. This spacecraft will be launched in 1998 and fly by an asteroid and a comet in 1999. Ion propulsion was considered an enabling technology for the Champollion comet sample return mission, which was recently selected as the fourth New Millennium mission and is slated for launch in 2003. Ion thrusters are also being studied for use in a Europa Orbiter mission and in the Pluto Fast Flyby. Mission designers require engine performance data over the throttling range to calculate the trajectory. Currently, the best estimate of end-of-life (EOL) performance is used for the whole trajectory to develop conservative mission designs. This requires EOL performance predictions which are guaranteed to be conservative, but not so conservative that mission objectives are unnecessarily sacrificed. Ideally, the effect of engine wear and aging processes on performance should be sufficiently well-understood that these conservatisms could be relaxed. Mission design could then be based on realistic estimates of the engine performance at any given time in the mission profile. The purpose of this research is to achieve this understanding.

NASA's 30 cm xenon ion thruster technology is being validated for use in near-Earth and planetary missions in the NASA Solar Electric Propulsion Technology Application Readiness (NSTAR) program. This program is designed to develop the industrial capability to produce flight engine, power processor and propellant feed system hardware and demonstrate that the technology is mature enough for flight applications. The technology validation portion of the program is focussed largely on providing flight program managers with sufficient information on performance, reliability and spacecraft interactions to allow them to use the technology.

The technology validation involves a large ground test program concentrating on the characterization of

engine performance as a function of time and power level, specification of the engine and plume interactions with the spacecraft, and understanding the dominant engine failure modes. The program includes anurnbe roflongduratio nteststoidentify unexpected failure modes, characterize the parameters which drive known failure mechanisms and determine the effect of engine wear on performance. In the first test, **2000 hours of operation at the full power point, several potential failure mechanisms were identified and studied** in subsequent shorter duration development tests. The effectiveness of design changes in essentially eliminating these failure modes was then validated in a 1000 hour wear test at the full power point, preparatory to starting an endurance test for the full 8000 hour design life. In this ongoing experiment, the most successful endurance test of a high power ion engine, a total of 6500 hours of operation have been achieved at the full power point. Engine performance changes, monitored continuously at the nominal operating point and periodically at throttled conditions, have been remarkably small at all but the lowest power levels. In this paper the performance changes will be presented and wear processes which appear to contribute to the changes will be identified.

Description of the Engine, Facility and Test Conditions

The Wear Test Engine

The endurance test is being conducted with the second Engineering Model Thruster (EMT2), fabricated by the Lewis Research Center (LeRC) [1, 2]. The discharge chamber of the 30-cm. diameter engine has a conical upstream segment and a cylindrical downstream portion. The magnetic circuit is a ring-cusp design with samarium-cobalt magnet rings located near the discharge cathode in the rear of the chamber, at the transition between the conical and cylindrical segments and at the upstream end near the ion optics. The two-grid, molybdenum optics and the hollow cathode technology are derived from the 30-cm, mercury engine development program, although the cathodes incorporate improved heater materials and handling procedures developed for the Space Station Plasma Contactor Program.

The flight engines being fabricated by the Hughes Electron Dynamics Division (HEDD) incorporate

several minor design changes which are not included in the EMT2 design. In the wear test engine the discharge chamber is fabricated from spun aluminum and titanium parts, while the flight design uses titanium for the entire discharge chamber. In addition, the gimbal bracket has been changed from stainless steel to titanium and some of the discharge chamber components have lightening holes in the flight design. Grit-blasted wire mesh which covers the upstream, conical portion of the discharge chamber for improved sputter containment in EMT2 has been extended to cover the downstream portion as well in the flight design. Many of the components in the flight thruster are being grit blasted to improve thermal radiation capability compared to EMT2. The flight design also uses slightly stronger magnets which have been thermally stabilized at a higher temperature. In EMT2 the main cathode keeper assembly is attached to the discharge chamber, while the flight design uses a brazed cathode-keeper assembly. These design changes have been validated by analysis or test and are not expected to negatively impact engine performance or wear characteristics.

Vacuum Facility and Support Equipment

The test is being conducted in a 3 m diameter, 10 m long stainless steel vacuum chamber pumped by three 1.22 m diameter CVI cryopumps with a pumping speed of about 45--50 kL/s on xenon and 3 xenon cryopumps consisting of 0.69 m² pure aluminum panels mounted on Cryomech AL200 coldheads with a pumping speed of about 18,000 l/s each, for a total speed of 100 kL/s. The development of the xenon cryopumps is discussed in more detail in [3]. This pumping system provides a no-load pressure of about $1-3 \times 10^{-5}$ Pa ($1-2 \times 10^{-7}$ Torr) and less than 5×10^{-4} Pa (4×10^{-6} Torr) at the full power flow rates. Approximately every 1000 hours these pumping surfaces must be regenerated, which exposes the engine to an atmosphere composed primarily of xenon at a pressure of about 4000 Pa (30 Torr). The cathodes are purged during these exposures and reconditioned after subsequent pumpdown to high vacuum. These events are usually accompanied by a short term (about 6 hour) increase in the high voltage recycle rate and temporary increase in the neutralizer keeper voltage and coupling voltage, but otherwise appear to have

no long term effects on engine operation.

To reduce the amount of facility material backspattered onto the engine, the walls and rear of the chamber are lined with graphite panels. The backsputter deposition rate, monitored with a quartz crystal microbalance (QCM) mounted next to the engine in the plane of the grids, is $0.16 \text{ mg/cm}^2\text{hr}$ or $0.7 \text{ }\mu\text{m/hr}$.

The propellant feed system used in the 1000 hour test [4] was modified for use in this test to include closed-loop flow control. This was accomplished by adding solenoid-driven micrometer valves in parallel with the manual micrometer valves used in the previous test. The manual valves provide a minimum purge flow during facility power outages and serve as a redundant flow control option in the event of a solenoid valve failure. All flow control valves are mounted inside the chamber, so that all external gas fittings have internal xenon pressures above atmospheric pressure to prevent leakage of air into the feed lines. The solenoid valves are driven by controllers with input signals from flow meters. This approach reduced the day-night fluctuations noted in the 1000 hour test [4]. The flow system is still subject to fluctuations of a few percent with a period of several minutes, which produce corresponding variations in the discharge voltage and current. Initial calibrations of the flow meters using three different calibration standards yielded results which agreed to within 1 percent. The flow meters are re-calibrated every 1000 hours and the flow meter zeroes are checked every 50-200 hours. The flow meter stability has been excellent, with responses generally varying by less than ± 1 percent.

The first 2974 hours of the wear test were conducted using a breadboard power processing unit (BBPPU) built by the Lewis Research Center which is described in detail in [5]. The test was continued using laboratory power supplies after the failure of the beam power supply in the BBPPU. These supplies are the same used in the 1000 hour test [4], although the accelerator grid power supply has been modified to permit high voltage recycles with the discharge current reduced to 4 A rather than 2 A. A second BBPPU has been fabricated and is now being installed for use in the remainder of the test.

Diagnostics

A computer data acquisition and control system is used to monitor facility and engine conditions and control the power supplies. Data are sampled and stored to disk once every 4-5 seconds. The system is programmed to turn off the engine if out-of-tolerance conditions in certain facility or engine parameters are detected to allow unattended operation. This system records engine electrical parameters measured to within ± 0.5 percent with precision shunts and voltage dividers and mean flow rates measured to within ± 1 percent with the thermal mass flow meters.

The thrust was measured directly in the first 3100 hours of the test using a modified version of the LeRC inverted pendulum thrust stand [6]. The thrust stand deflection, measured with a linear variable differential transducer (LVDT), was calibrated in-situ by applying small weights. Long-term drift in the thrust stand response was on the order of 1 percent. At each of the measurements, conducted every 50-200 hours, ten thrust stand calibrations were performed. The short-term repeatability of the response in these calibrations was within 0.6 percent. Additional uncertainties in the measurement of the LVDT voltage yield a total uncertainty in the thrust measurement of about ± 1.5 percent. At 3100 hours a failure in the closed loop control of the thrust stand inclination left the thrust stand inoperable.

The ion beam characteristics are measured with near- and far-field probes. The near-field Faraday probe is a 0.8 cm diameter molybdenum disk mounted on an arm that can be swung through the beam at distance of about 2.5 cm downstream of the ion extraction system. The probe is biased -20 V with respect to facility ground to repel electrons. A probe consisting of an array of rods mounted at the end of the chamber is used primarily to monitor the behavior of the thrust vector. The square array is composed of 16 vertical and 16 horizontal graphite rods, each 9 mm in diameter and 1.2 m long. The rods are also biased -20 V to repel electrons, so the current measured by each rod represents the integral of the ion current density distribution at one lateral (vertical or horizontal) position across the beam. The lateral integrated profiles can be fit with gaussian distributions, as Fig. (1) shows. The intersection of the centroids of these distributions defines the location

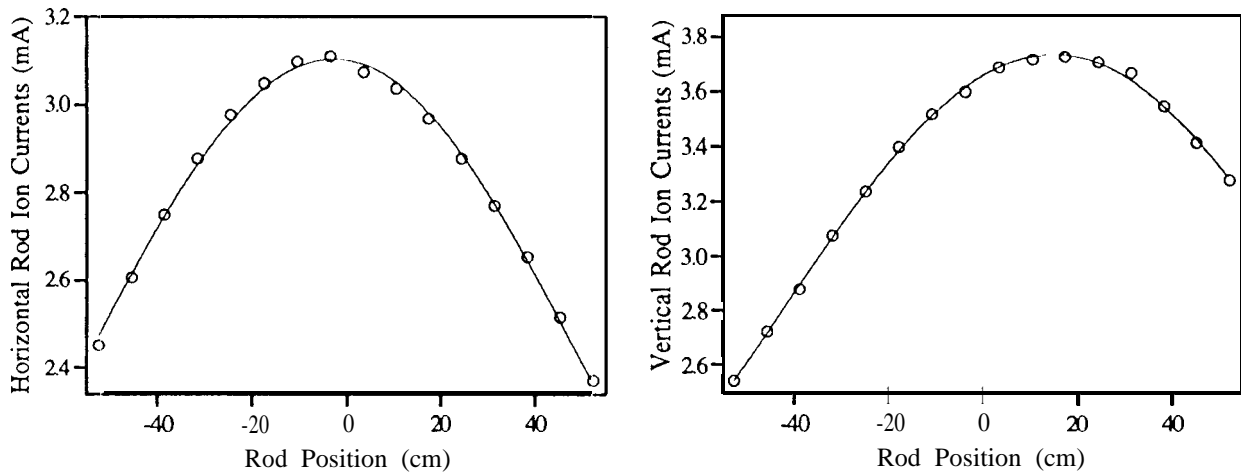


Figure 1: Measures of beam spread using the thrust vector probe array.

of the thrust vector. Because the inclination of the thrust stand could be varied over a range of one degree and reassured by an inclinometer with a resolution of better than 0.001 degrees, it was possible to actively sweep the beam across the thrust vector probe in one axis. The beam centroid measurements agreed with the inclinometer measurements to within 2 percent and demonstrated that the thrust vector probe has an angular resolution of 0.01 degrees. For this discussion, however, the capability of measuring the beam spread with the probe is more important. The widths of the gaussian distributions of integrated current density in each axis are generally very similar, indicating that the beam current density distribution is axisymmetric and follows a gaussian distribution with the same width. The effect of charge exchange ions on the distributions was studied in initial tests with a stainless steel mesh covering the probe. The mesh was biased negative to filter electrons, while the rods were biased positive to repel low energy charge exchange ions. These measurements indicated that the charge exchange ions normally collected by the rods tend to broaden the current density distribution. This effect prevents absolute measurements of the beam spread, but measurements performed while varying the beam voltage demonstrate that the probe is insensitive to significant changes in beam divergence.

The double-to-single ion current ratio is monitored periodically with an ExB probe mounted in the rear of the chamber. This ion velocity filter is described in

more detail in references [4, 7]. The collimating slits on this probe permit ions emitted from a strip 3.1 cm wide extending across the entire face of the ion engine to be sampled, so the measured current ratio represents the integral of the current ratio distribution across the thruster. Charge exchange reactions in the beam may also influence the ratio measurements, but no corrections for this effect have been made.

Measurements of the grid perveance limit and electron backstreaming limit taken every 50-200 hours are used to monitor changes in ion optics performance and provide an indirect measure of changes in accelerator grid aperture sizes. Hole diameters can be measured directly using a laser profilometer and small video cameras mounted on a positioning system in the vacuum chamber. The laser profilometer, which has a resolution of $1 \mu\text{m}$ over a range of $400 \mu\text{m}$, is used to define the downstream edge of an aperture in three locations, from which the downstream diameter is estimated. The hole wall can be illuminated by the laser at only one azimuthal location, so the profilometer cannot be used to measure the minimum diameter at the chemical etch cusp. However, this diameter can be estimated from video images of the grid with the holes backlit using lights on the positioning system. These measurements have been performed at several radial locations about once every 1000 hours but are still being analyzed.

The screen grid, which is normally connected elec-

<i>Controlled Parameters</i>	Nominal Test Point	Throttle Points					
		1	2	3	4	5	6
Beam Supply Voltage, V	1100	1100	1100	1100	1100	1100	650
Beam Current, A	1.76	1.76	1.59	1.26	1.01	0.66	0.54
Accelerator Voltage, V	-180	-180	-180	-180	-180	-150	-150
Neutralizer Keeper Current, A	1.5	1.5	1.5	1.5	1.5	1.5	1.5
Main Flow Rate, seem	23.7	23.2	21.6	16.8	12.5	8.0	6.0
Cathode Flow Rate, seem	3.7	3.0	2.5	2.1	2.1	2.1	2.1
Neutralizer Flow Rate, seem	3.0	3.0	2.5	2.1	2.1	2.1	2.1
<i>Dependent Parameters</i>							
Beam Voltage, V	1088	1091	1092	1096	1091	1093	634
Accelerator Grid Current, mA	8.6	9.4	7.1	4.6	3.2	1.7	1.5
Discharge Voltage, V	25.1	26.0	26.0	25.5	26.0	27.1	27.9
Discharge Current, A	12.8	11.8	10.4	9.1	8.1	5.3	4.8
Neutralizer Keeper Voltage, V	14.3	14.2	14.7	15.7	17.1	19.4	21.2
Coupling Voltage, V	-13.4	-13.8	-14.2	-14.2	-14.2	-13.9	-13.6
Power, kW	2.32	2.27	2.05	1.66	1.35	0.90	0.51
<i>Performance</i>							
Thrust, mN	92.6	92.5	83.8	66.9	52.8	34.8	21.6
Specific Impulse, s	3170	3300	3290	3330	3300	2900	2200
Efficiency	.63	0.66	0.65	0.65	0.64	0.56	0.45
Discharge Loss, eV/ion	173	174	170	182	209	215	247
Propellant Efficiency	0.89	0.94	0.92	0.94	0.97	0.91	0.93

Table 1: Independent engine parameters and beginning-of-life dependent parameters and performance values

trically to the discharge cathode, is periodically biased 20 V negative of cathode potential to measure the ion current collected by it. From these measurements the screen grid transparency to ions is determined.

Test Conditions

The power supply setpoints (measured at the thruster) and flow rates for the nominal full power operating point are listed in Table (1) with the beginning of life values of the dependent electrical and calculated performance parameters. These conditions, which match those of the 1000 hour test, have been maintained for most of the endurance test. Every 1000 hours engine operation is characterized over the full power range at the six throttle points listed in Table (1). These do not correspond exactly to the current NSTAR throttling profile, but are used as standard test conditions to allow comparisons with

previous data. Periodically other off-nominal operating conditions are tested to guide development of the throttle table or study particular phenomena, such as engine sensitivity to small variations in the controlled parameters [8].

Performance Changes at the Nominal Operating Point

The three performance parameters of interest to mission designers are thrust, specific impulse and efficiency. The thrust is given by

$$T = \alpha F_t J_b V_b^{1/2} \left(\frac{2M}{e} \right)^{1/2} \quad (1)$$

where J_b is the beam current, V_b is the net accelerating voltage, M is the mass of a xenon ion and e is the charge of an electron. The factors α and F_t correct for the doubly-charged ion content of the beam and thrust loss due to non-axial ion velocities. The

double ion correction factor is expressed as

$$\alpha = \frac{1 + J^{++}/\sqrt{2}J^+}{1 + J^{++}/J^+} \quad (2)$$

where J^+ / J^+ is the mean ratio of doubly- to singly-charged ion current. The beam divergence correction is given by the expression

$$F_t = \frac{\int_{\theta_{min}}^{\theta_{max}} (J^+ + J^{++}) \cos \theta d\theta}{\int_{\theta_{min}}^{\theta_{max}} (J^+ + J^{++}) d\theta} \quad (3)$$

in which θ is the angle from the centerline. The thrust will therefore vary as engine wear affects the beam current, beam voltage, double-to-single ion current ratio or beam divergence. The specific impulse will change as the thrust decays or propellant flow rate changes. Finally, the overall efficiency will change over the engine life as the thrust drops at a given power level, as the power required to maintain a certain thrust increases, or as flow rates change.

Figure (2) displays the measured thrust, calculated thrust and beam current at the nominal operating point over 6500 hours of operation. The calculated thrust is based on the measured beam current and voltage, a constant value of 0.98 for F_t and a value of α based on a curve fit to centerline double ion current measurements as a function of propellant utilization efficiency in a 30 cm, ring-cusp inert gas thruster[9]. The uncertainty in the calculated values is on the order of ± 2.1 percent. Given the uncertainties in the measured and calculated values the agreement is quite good. The measured and calculated thrust decreased slightly between 1000 and 2200 hours as the beam current dropped from 1.76 A to 1.75 A. This was due to a software discharge current limit in the BBPPU which prevented operation above 14 A. Over this time period this limit made it impossible to maintain the beam current setpoint. When the software was modified at 2200 hours to permit higher discharge currents the beam current and thrust returned to the previous values. In general, however, the thrust is quite constant over the first 3000 hours, varying by ± 1 mN about a mean of 93.4 mN.

Although there are no direct thrust measurements after the first 3000 hours, it appears that the thrust has remained essentially unchanged. The beam current and net accelerating voltage have been set at

fixed values and the double-to-single ion current ratio has remained constant at 0.20 ± 0.01 after increasing from about 0.15 in the first 1000 hours, as shown in Fig. (3). These measurements are integrated across a thruster diameter, so they overestimate the average double-to-single ion current ratio. Detailed data from the J-series 30 cm mercury thrusters suggests that the average value is 0.34 --0.5 times the integrated ratio[10], which yields an average ratio of .07--0.1 for this engine. Figure (4) displays the width of the gaussian distributions fit to the thrust vector probe data in the vertical and horizontal axes as a function of time. The fact that the beam spread recorded by the array has varied by less than 1 percent over the entire 6500 hours suggests that no significant changes in the thrust loss due to divergence have occurred. The Faraday probe also shows no significant changes in the near-field beam profile over the course of the test.

The specific impulse has also apparently not varied during the test, because the thrust has been constant and the flow rates are controlled. The efficiency, however, dropped by one percentage point in the first 3000 hours as the engine power required to produce the commanded beam current increased from 2290 W to 2320 W, as shown in Fig. (5). The beam power is controlled, so the increased demand is solely due to increases in discharge power. This is reflected in the ion production cost, which is plotted in Fig. (6). The ten percent growth in discharge losses is confined to the first 3150 hours, after which it has remained constant at about 200 eV/ion. The plots of discharge current and voltage in Fig. (7) show that most of the increase in discharge power was due to an increase in the discharge current. After about 3100 hours the discharge voltage started to drop slightly. This was compensated by further increases in the discharge current. Both voltage and current have been relatively constant since hour 5'200. It is remarkable that the engine continues to run so efficiently with such a low discharge voltage. The performance changes at the full power operating point, fortunately, have been quite small.

Performance Changes at Throttled Conditions

Throttling tests have been conducted approximately every 1000 hours. In these tests the controlled

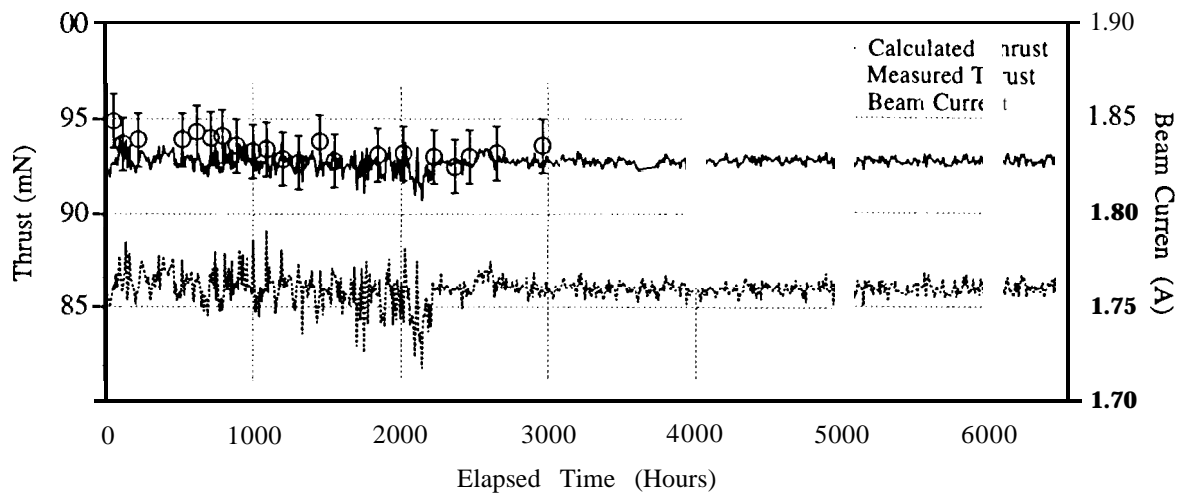


Figure 2: Measured thrust, calculated thrust and beam current at the nominal operating point.

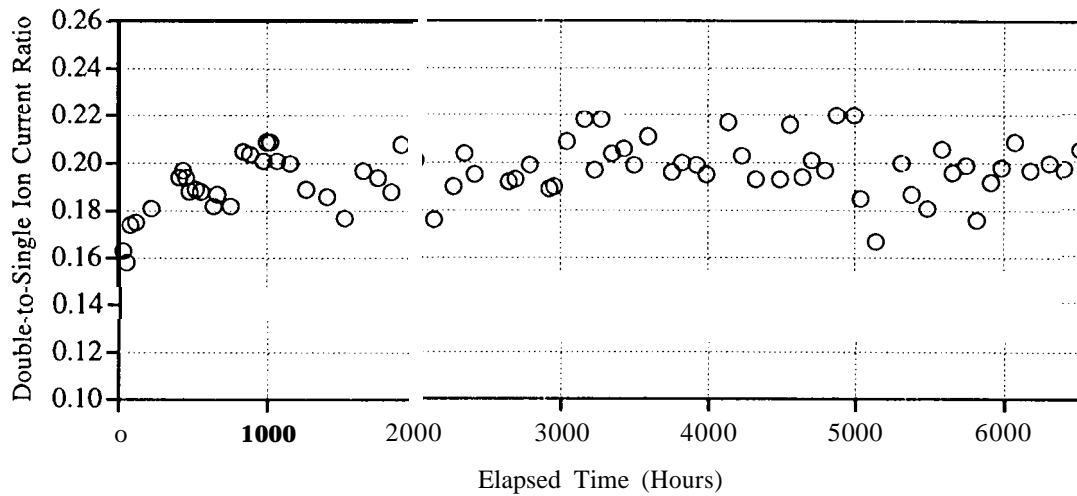


Figure 3: Double-to-single ion current ratio measured with the ExB probe.

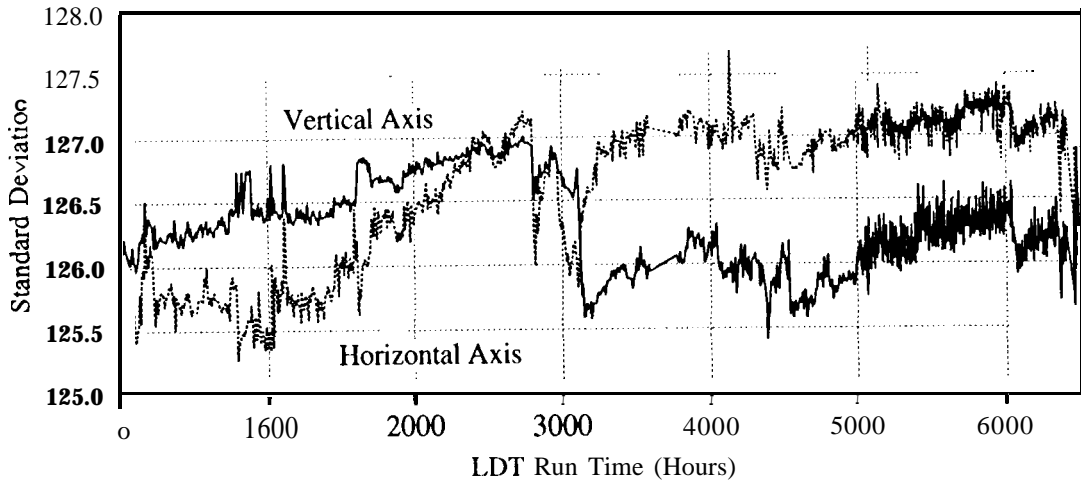


Figure 4: Variation in the width of the beam profile measured with the thrust vector probe.

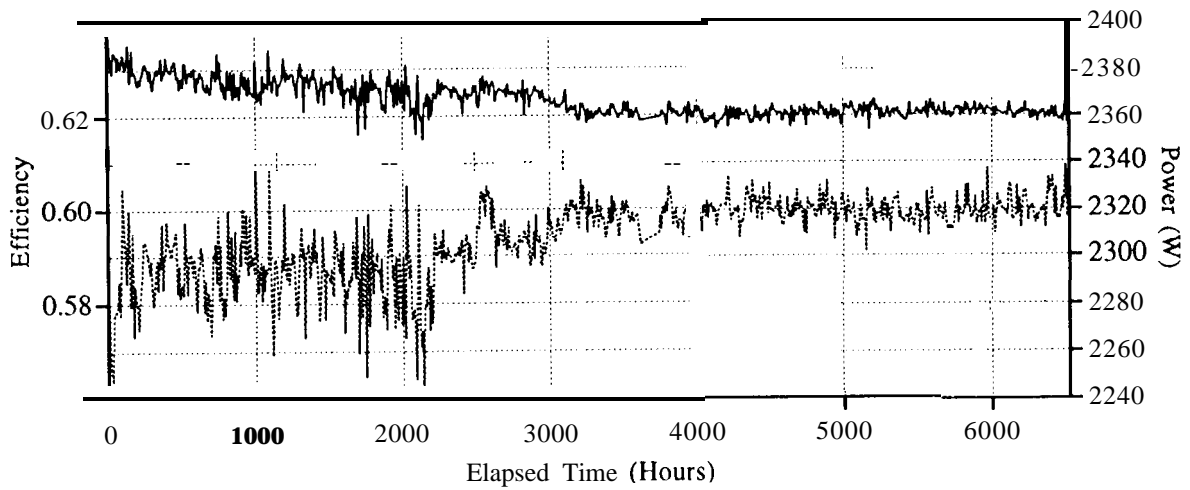


Figure 5: Efficiency and power as a function of time for the nominal operating point.

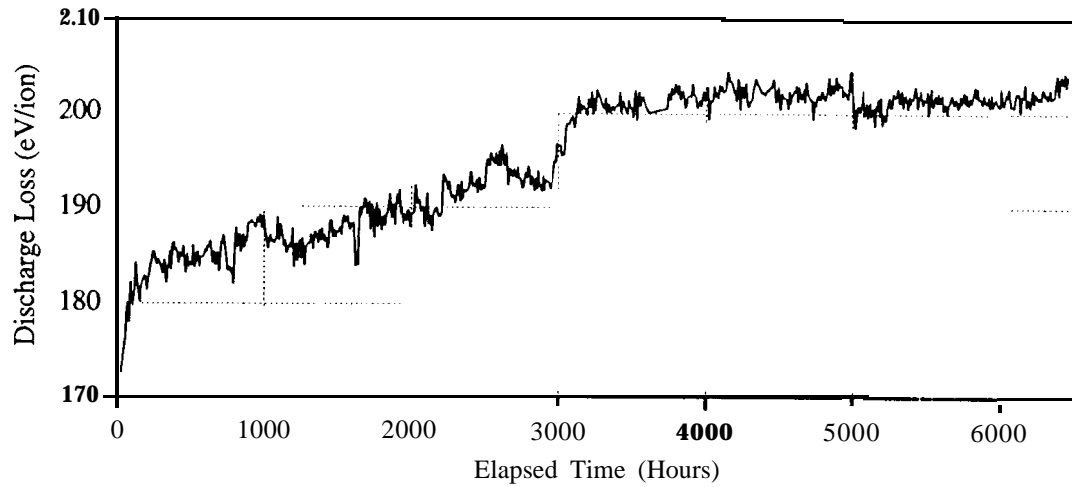


Figure 6: Increases in ion production cost are responsible for growth in power requirement.

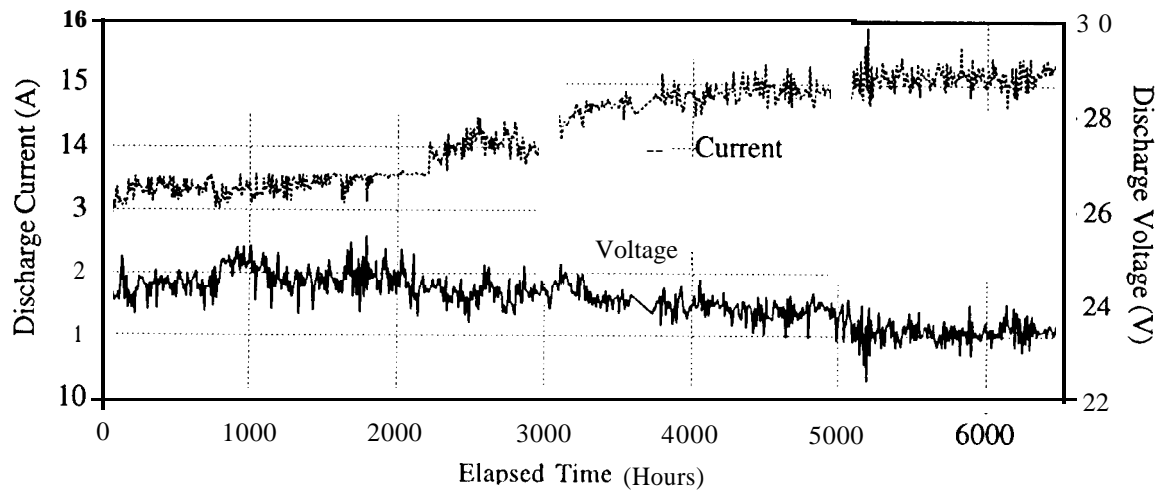


Figure 7: Variations in discharge current and voltage over the course of the test

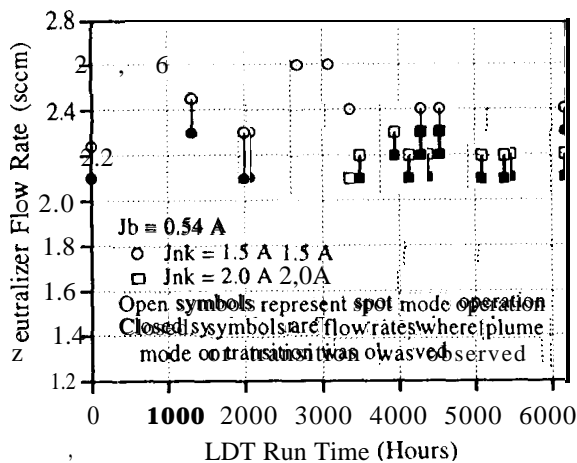


Figure 8: The transition from plume to spot mode as a function of neutralizer flow rate, keeper current and time.

engine parameters were all fixed at the values listed in Table (1) with the exception of the neutralizer flow rate and keeper current. As the wear test progressed it became necessary to increase the neutralizer flow rate and keeper current at the two lowest throttle points to maintain spot mode operation. Data on the transition from spot mode to plume mode are presented as a function of time for the minimum power point in Fig. (8). In this plot the transition is defined as the flow rate at which the neutralizer keeper voltage oscillations exceed 5 Vp-p. These and other data from neutralizer characterizations suggest a shift in neutralizer behavior sometime between 1400 and 2000 hours. No facility-related test events or periods of off-nominal operation that could explain the shift have been identified in this period, so it is currently assumed conservatively that this is indicative of normal wear. The flow rates and currents used in the throttling tests are plotted in Fig. (9). The 2.6 sccm flow rate used in the tests at 3100 hours is apparently more than necessary to avoid plume mode operation; a lower value was adequate in subsequent tests.

The thrust as a function of power level is shown in Fig. (10). The values measured at the beginning of the test are systematically higher by 1-2 percent, which is excellent agreement given the uncertainties

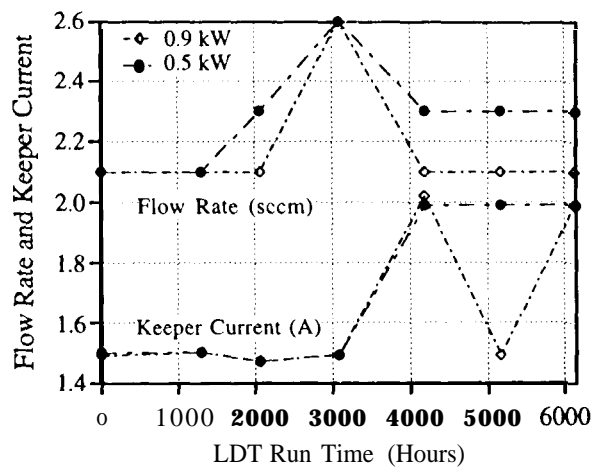


Figure 9: Neutralizer flow rates and keeper currents used in the throttling tests.

in the measurements. The calculated thrust was essentially constant as a function of time, because the engine operating conditions which enter the thrust calculation were controlled. The power required to deliver that thrust increased with time, however, as the figure demonstrates. The ratio of double-to-single ion current as a function of time for the six throttle points is shown in Fig. (11). For the three lowest throttle points the ratio has been approximately constant, while it increased by about 50 percent over the first 3000 hours for the three highest power levels. Because this behavior is different from that observed at the nominal test point, the engine was operated at the throttle test full power point for 90 hours to verify that it was not a transient effect associated with throttling down the engine. The ratio was stable at the higher value for this entire period, confirming the measurements made in the shorter duration throttling tests. This increase in the double ion content could be responsible for a decrease in thrust of up to 1 percent, when the ratios of double-to-single ion current integrated over a thruster diameter are corrected to average ratios using the method discussed in [10]. The spread in the gaussian beam profiles measured with the thrust vector probe changed in general by less than 1-2 percent over time, indicating that the beam divergence has not changed dramatically. The

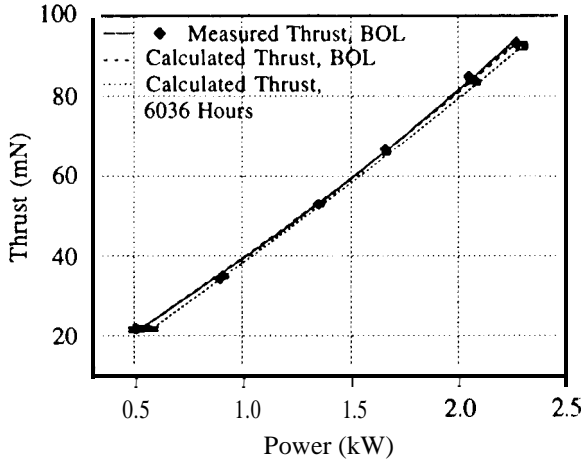


Figure 10: Thrust as a function of power level for the points used in the throttling tests.

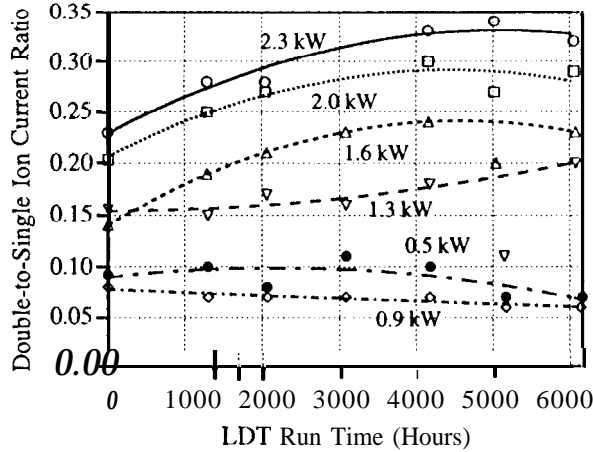


Figure 11: Double-to-single ion current ratios measured in the throttling tests.

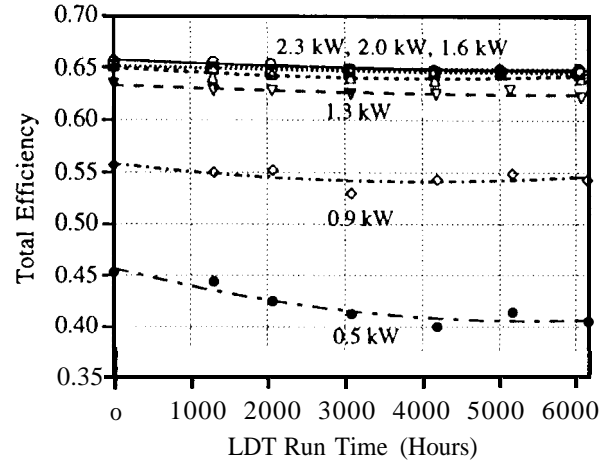


Figure 12: Efficiency as a function of time and power level for the throttle test points.

true thrust is therefore likely to have remained near the calculated values.

The increase in power for a given thrust implies a lowering of the overall efficiency, as shown in Fig. (12). The efficiency losses are less than 1.5 percentage points for all but the lowest power level, at which a loss of 4 percentage points has occurred. This is due in part to the higher neutralizer flows required at the lowest power, although this represents only about 0.9 percentage points of the total 4. As with the nominal full power test point, the efficiency decline is mainly due to increased discharge power requirements, as Fig. (13) shows. The greatest increase in beam ion production cost was experienced at the lowest power level. This curve also shows the largest scatter in the measurements. These data and those at the nominal operating point suggest that engine wear experienced in this test has had a negligible impact on performance at higher power levels but has resulted in significant losses at the lowest power level.

The Effect of Engine Wear on Performance

The observed behavior can be interpreted qualitatively with the use of a discharge chamber performance model developed in [11]. In this formulation the beam ion production cost is given by

$$\epsilon_B = \frac{\epsilon_P^*}{f_B [1 - e^{-C_0 \dot{m} (1 - \eta_w)}]} + \frac{f_C V_D}{f_B}, \quad (4)$$

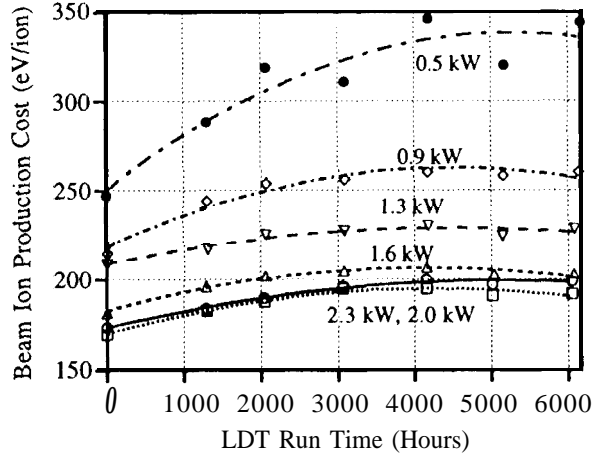


Figure 13: Discharge losses as a function of time and power level for the throttle test points.

where $f_B = J_B/J_P$ is the beam current divided by the total ion production rate expressed as a current, $f_C = J_C/J_P$ is the fraction of all ions produced that are collected on cathode potential surfaces, \dot{m} is the mass flow rate into the discharge chamber, η_u is the propellant utilization efficiency and V_d is the discharge voltage. The total ion production rate is the sum of the beam current, the ion current to anode potential surfaces and the ion current to cathode potential surfaces,

$$J_P = J_B + J_A + J_C \quad (5)$$

The baseline plasma ion energy cost ϵ_P^* is

$$\epsilon_P^* = \frac{\epsilon_0 + \epsilon_M}{1 - (V_C + V_D)/V_D}, \quad (6)$$

in which ϵ_0 represents the average energy expended per plasma ion in ionization and excitation reactions and ϵ_M is the average energy of a Maxwellian electron lost to the anode. The primary electrons are assumed to be injected into the discharge plasma from a potential which is V_C volts above cathode potential, so V_C represents the voltage associated with cathode operation. The primary electron utilization factor C_0 represents the extent to which primary electrons interact with the neutrals, and is given by

$$C_0 = \frac{4\sigma'_0 l_e}{e v_0 A_g \phi_0}, \quad (7)$$

where σ'_0 is the total inelastic collision cross section, l_e is the primary electron containment length, v_0 is the thermal velocity of the neutrals, A_g is the active grid area and ϕ_0 is the transparency of the ion optics to neutral atoms. This model has been shown to accurately predict the variation in plasma ion energy cost for changes in propellant, grid transparency to neutral atoms, beam extraction area, discharge voltage and discharge chamber wall temperature [11]. The experiments show that the four parameters which determine discharge chamber performance, f_B, f_C, C_0 and ϵ_P^* , are largely independent of the flow rate and the propellant utilization for a wide range of conditions. At low discharge voltages, however, the baseline plasma ion cost ϵ_P^* starts to show a dependence on flow rate. This is evidently due to variations in the electron temperature, and thus the Maxwellian electron energy ϵ_M , with flow rate, which has a greater impact on ϵ_P^* when the discharge voltage is low.

The four parameters which govern discharge chamber performance are dependent on engine characteristics which can change as the engine wears. The primary electron utilization factor C_0 depends on the grid transparency to neutral atoms, so accelerator or screen grid wear which increased the aperture diameters would lead to a performance decrease due to greater neutral losses. The primary electron containment length l_e is determined largely by the configuration and strength of the magnetic field. Therefore thermal degradation of the magnets could result in performance losses by its effect on l_e . The magnitude of the total inelastic collision cross section σ'_0 is determined by the primary electron energy, which depends on the discharge voltage. Variations in voltage over lifetime might therefore influence this parameter. Finally, C_0 is sensitive to the neutral atom thermal velocity, so if the discharge chamber temperature rises the performance will suffer. This behavior can be seen on a short time scale; the ion production cost increases over the first hour or so after ignition as the engine temperature rises to its steady state value. This could also happen over longer time scales as other processes make the discharge less efficient and more energy is deposited in the structure.

The baseline plasma ion energy cost is sensitive primarily to the electron temperature through its effect on ϵ_M and on cathode operation through V_C . Processes which lead to higher electron temperatures

would therefore decrease performance, as would cathode degradation which resulted in an increase in V_c .

The fraction of ion current to cathode potential surfaces f_C is the sum of the screen grid current and the ion current from the discharge plasma to the cathode and is likely dominated by the current to the screen grid because of the larger area. Grid wear processes which affect the screen grid transparency to ions will therefore affect this fraction. For a constant beam current, the extracted ion fraction f_B will drop only as the total ion production rate rises. Increased ion fluxes to the screen grid, cathode or anode will reduce discharge chamber performance. This might occur through grid erosion or changes in the magnetic field strength.

It is clearly very difficult to measure certain model parameters such as the ion current collected by the anode. In addition, there are no detailed maps of the discharge chamber plasma for the NSTAR engine, so a number of the plasma properties are unknown. This makes it impossible at this point to quantitatively apply the model to interpret the observed performance changes. However, there is evidence of wear processes that are consistent with the effects outlined above.

The perveance and electron backstreaming limit measurements provide an indirect method of monitoring changes in the accelerator grid aperture diameters. The perveance limit, defined as the voltage at which the accelerator grid current changes 0.02 mA for every volt change in beam supply voltage, is plotted for the nominal operating point in Fig. (14). The electron backstreaming limit, defined by a 1 percent decrease in discharge loss due to backstreaming, is shown in Fig. (15) for the nominal operating point. The perveance data indicate a relatively steep change in the limit over the first 1000 hours and an approximately constant, although slower, decrease after that. The electron backstreaming limit measurements show a more or less constant increase in the magnitude of the accelerator grid voltage required to prevent backstreaming. Similar measurements taken during the throttling tests show the same behavior. Both data sets are consistent with an increase in accelerator grid hole diameter due to sputter erosion from the impact of charge exchange ions generated in the interelectrode gap or the aperture itself. As the model shows, this can lead to higher discharge losses because of a decrease in the primary electron

utilization factor from a higher grid transparency to neutrals. These measurements do not yield a quantitative value for the change in hole diameter, but the profilometer and grid image data should allow the change in transparency to be estimated.

The ion current collected by the screen grid represents an energy loss to the discharge plasma which is captured in this model by the parameters f_C and f_B . This effect is quantified in Fig. (16), which shows the measured ion current to the screen grid as a function of time for the nominal operating point. These data indicate an increase in screen grid current of 60 mA, a 16 percent change since the beginning of the test. Similar results were obtained in the throttling tests at lower power levels. Most of this increase occurs in the first 3200 hours, which is consistent with the performance changes. This suggests this effect may dominate over the increased grid transparency to neutrals, which has continued to rise while the performance has essentially stabilized. The two may be related, however. The decreased screen grid transparency to ions may be due to changes in the upstream sheath shape caused by an increase in the accelerator grid aperture sizes.

Thermal degradation of the magnets is not thought to be a significant contributor to the observed effects. Development tests of the samarium-cobalt magnets used in this design have shown very little decrease in the magnetic field strength after long periods of operation at elevated temperatures. In addition, the near-field beam probe results suggest no major changes in the plasma distribution, which should be sensitive to magnetic field strength in the discharge chamber.

There are no direct measurements of the cathode voltage V_C or the electron temperature, but the cathode keeper voltage data suggest that one of these parameters is changing. The keeper voltage is displayed in Fig. (17) with the discharge voltage. The keeper is electrically connected to the anode with a 1 kOhm resistor, and draws approximately 20 mA of electron current. The potential of the keeper is therefore sensitive to both the local plasma potential and the electron temperature. A drop in the local potential or an increase in the electron temperature would explain the voltage decrease observed in the test. The fact that the discharge voltage is also decreasing suggests the former. A lowering of the potential near the cathode could signal more efficient cathode operation,

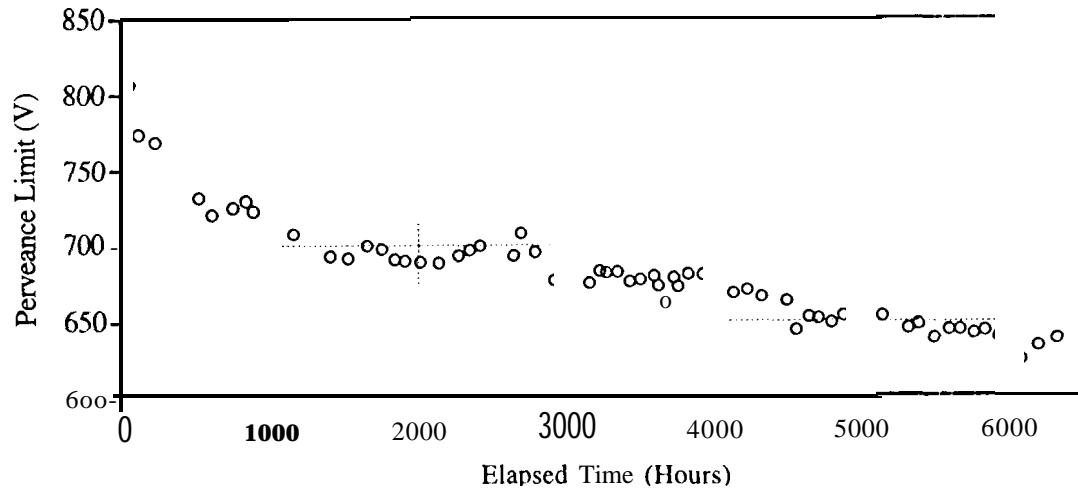


Figure 14: Perveance limit measurements obtained over the course of the test.

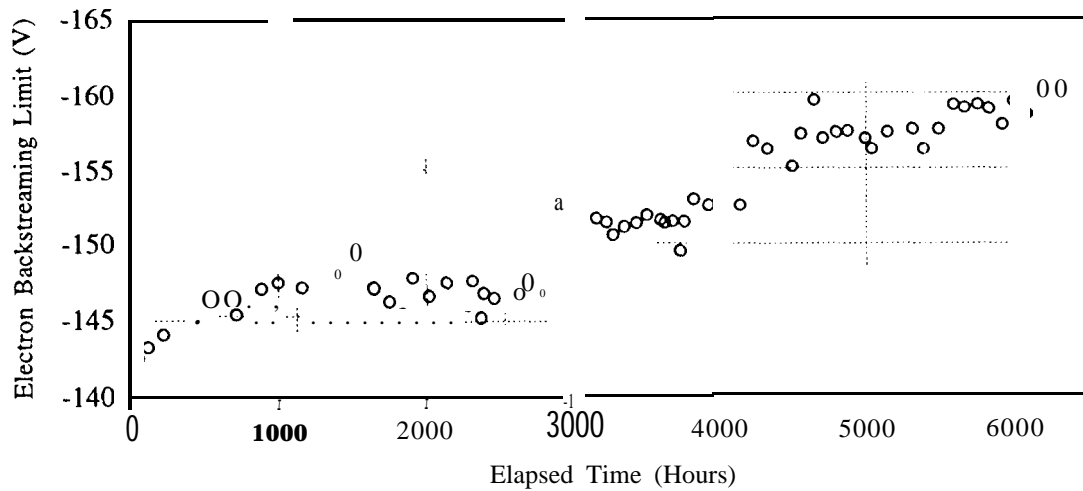


Figure 15: Variations in the electron backstreaming limit over time.

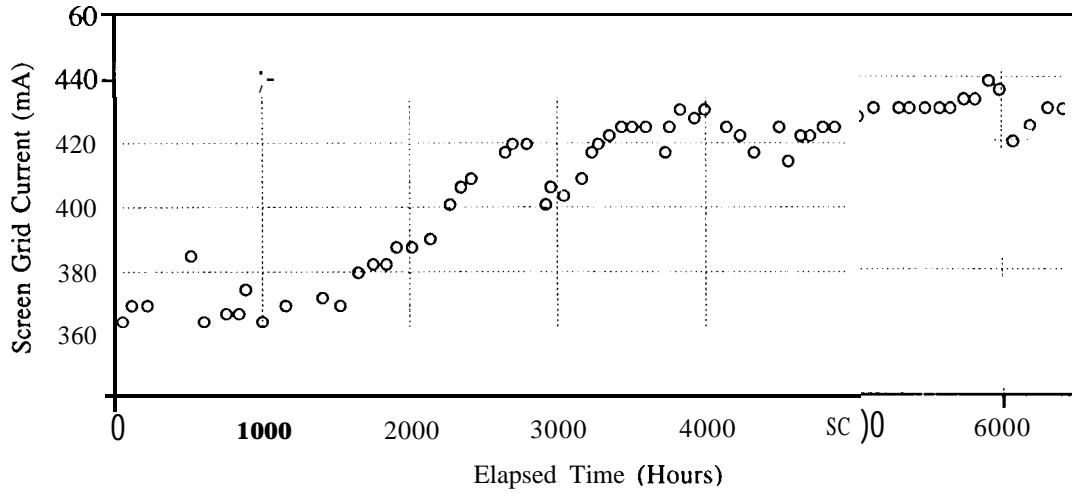


Figure 16: Increases in screen grid current observed over time.

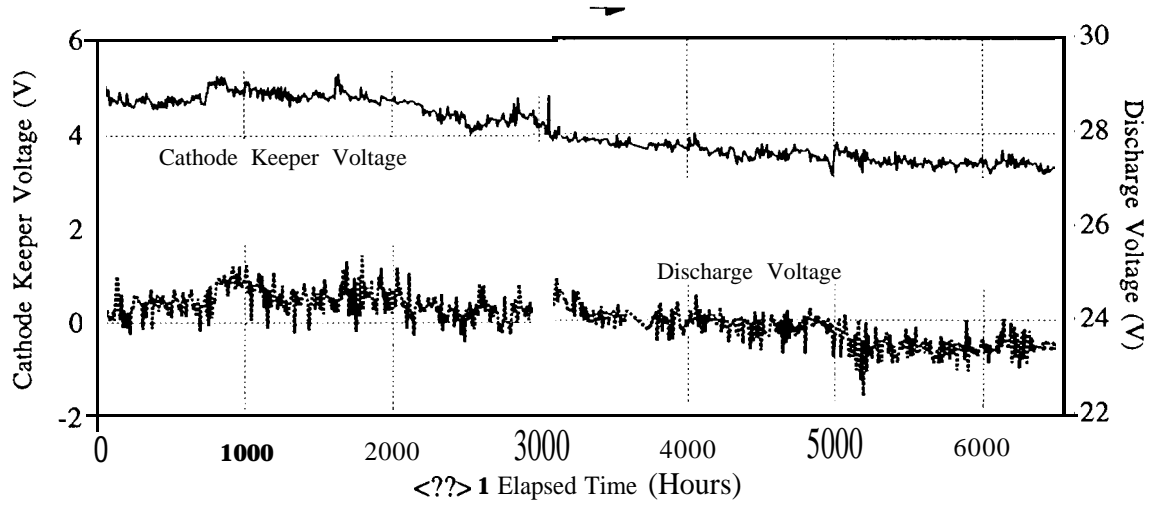


Figure 17: Variations in cathode keeper and discharge voltage over the course of the test.

perhaps because of the higher discharge current.

Finally, the discharge chamber wall temperature has likely increased some simply because the discharge losses are higher. This could magnify the performance loss by increasing the neutral atom velocity and decreasing Co. A number of these issues will be resolved with further testing and analysis. For example, the image data and post-test examinations will quantify changes in aperture diameters and indicate over what period of time the changes occurred. Similarly, the post-test analysis will show whether significant changes to the magnets have occurred. In addition, by measuring the discharge loss, discharge voltage, beam current and screen grid current (which is approximately equal to J_C) for a range of neutral density parameters $\dot{m}(1 - \eta_u)$, it should be possible to determine the ratio ϵ_P^*/f_B and Co in Eq. (4) by non-linear regression. Resolving these parameters in this way would be very interesting because it would provide separate reassures of the response to increases in grid transparency to neutrals (through C_0) and decreases in the extracted ion fraction (through ϵ_P^*/f_B). In subsequent tests such measurements should be made periodically to determine how these parameters change with time. Additional instrumentation in these tests, such as discharge chamber temperature sensors and magnetometers to monitor the magnetic field strength, would provide valuable information about the effect of wear on engine performance.

The Effect of Flow Rate on Performance and Sensitivity to Wear

The data show only small changes in performance at all power levels except the lowest, where a significant decrease is observed. The discharge chamber performance model shows that this can be explained by the throttled flow rates required for lower power operation. Differentiating Eq. (4) with respect to C_0 and J_C/J_B yields the sensitivity of the discharge loss to the processes identified above. The sensitivity to increased neutral losses is given by

$$\frac{\partial \epsilon_B}{\partial C_0} = \frac{\epsilon_P^* \dot{m} (1 - \eta_u) e^{-C_0 \dot{m} (1 - \eta_u)}}{f_B [1 - e^{-C_0 \dot{m} (1 - \eta_u)}]^2} \quad (8)$$

If Co is small, the exponential terms dominate and give an increase in sensitivity to changes in C_0 with decreasing flow rate. A similar, but weaker effect is

found for the sensitivity to changes in the ion current to cathode potential surfaces relative to the beam current,

$$\frac{\partial \epsilon_B}{\partial (J_C/J_B)} = \frac{\epsilon_P^*}{1 - e^{-C_0 \dot{m} (1 - \eta_u)}} + V_D. \quad (9)$$

Changes in screen grid current which produce negligible effects at high flow rates can produce much larger changes in ϵ_B at reduced flows. These are significant results, because the power profiles for many outbound planetary missions such as DS-1 demand long periods of operation at low power levels,

The sensitivity of the beam ion production cost to small variations in the flow rate about the nominal value can also be examined with this model. This sensitivity is given by

$$\frac{\partial \epsilon_B}{\partial \dot{m}} = \frac{\epsilon_P^* C_0 (1 - \eta_u) e^{-C_0 \dot{m} (1 - \eta_u)}}{f_B [1 - e^{-C_0 \dot{m} (1 - \eta_u)}]^2} \quad (10)$$

This shows unambiguously that the sensitivity to flow rate variations increases as the nominal flow rate decreases, which may explain the scatter in the measurements of ϵ_B at the lowest power level. Small variations in the flow rates from test to test can cause significant variations in the discharge performance. This behavior was confirmed experimentally in sensitivity tests performed during the wear test, as shown in Fig. (18). This essentially represents a shift in the knee of the performance curve to lower propellant efficiencies as the flow rate is reduced, which suggests that to maintain optimum performance the propellant efficiency must decrease as the flow is reduced. This was found to be true in recent low power throttling tests, which showed optimum total efficiencies at propellant utilization efficiencies between 0.8 and 0.85.

Conclusions

Performance changes have been negligible at the nominal full power operating point in the NSTAR 8000 hour wear test and at all but the lowest power level of the six throttle points measured periodically during the test. At the minimum power point the performance degradation is not insignificant, representing a 9 percent loss in efficiency (4 percentage points out of 45 percent). The observed decrease in

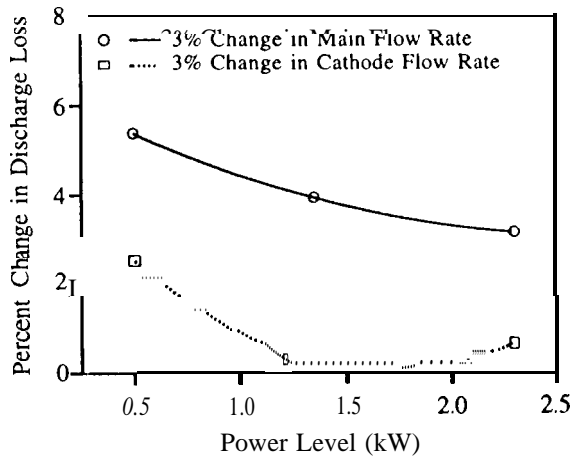


Figure 18: Variations in discharge loss for small variations in flow rate as a function of power level.

efficiency at the higher power levels is due primarily to an increase in the discharge losses. At the minimum power point the efficiency has suffered slightly from increased neutralizer flows required to maintain spot mode emission as the test has progressed, but the dominant effect on the performance is also an increase in the beam ion production cost. A model of discharge chamber performance which predicts the ion production cost yields insights into what wear or aging processes can affect engine performance. Periodic measurements in the wear test have documented evidence of accelerator grid hole enlargement which can lead to greater neutral losses and increased ion current to the screen grid. These two effects both lead to increased discharge power requirements to maintain a given beam current. The model also shows that the performance impacts of these wear processes are greatest at low flows, giving a qualitative explanation of the insensitivity at the higher power levels.

Previous end-of-life performance projections for mission planning involved extrapolation of data from the endurance test, and then sampling from bounds on certain parameters and using the sensitivity data to estimate uncertainties in the projected performance. Now that the engine in the wear test has processed as much propellant as the flight thruster will during the DS-1 mission, measurements taken over the throttling range are being considered end-of-

life values. Both of these approaches are suspect; the first because it involves extrapolation without knowing the true functional form of the temporal variations and the second because the engine wear does not scale strictly with amount of propellant processed. Ideally the endurance test experience should be used to determine which wear processes affect which performance parameters, and then couple a performance model with wear models to calculate performance over mission profile. Preliminary results from the test to-date provide the first steps toward achieving this capability.

Acknowledgements

The authors would like to acknowledge the invaluable fabrication and test support provided by LeRC's Test Installations Division as well as Al Owens, Bill Thogmartin and Bob Toomath at JPL. The support of other NSTAR Project members including Jack Stocky (JPL), Frank Curran and John Hamley (LeRC), Keith Good fellow, Mike Marcucci, Dave Brinza, Mike Henry and Mike Smith (JPL) and Roger Myers (previously with NYMA, Inc.) is also gratefully acknowledged. The research described in this paper was conducted in part at the Jet Propulsion Laboratory, California Institute of Technology, and was sponsored by the National Aeronautics and Space Administration.

References

- [1] M.J. Patterson and T. Haag. Performance of the 30-cm Lightweight Ion Thruster. In *23rd International Electric Propulsion Conference*, Seattle, WA, 1993. AIAA-93-108.
- [2] J. S. Sovey et al. Development of an Ion Thruster and Power Processor for New Millennium's Deep Space 1 Mission. In *33rd Joint Propulsion Conference*, Seattle, WA, 1997. AIAA-97-2778.
- [3] J.R. Brophy C.E. Garner, J.E. Polk and K.D. Goodfellow. Methods for Cryopumping Xenon. In *32th Joint Propulsion Conference*, Lake Buena Vista, FL, 1996. AIAA-96-3206.
- [4] J.E. Polk et al. A 1000-Hour Wear Test of the NASA NSTAR Ion Thruster. In *32nd Joint*

- Propulsion Conference, Lake Buena Vista, FL, 1996. AIAA-96-2717.
- [5] J. A. Hamley et al. Development Status of the NSTAR Ion Propulsion System Power Processor. In 31st *Joint Propulsion Conference*, San Diego, CA, 1995. AIAA-95-3305.
- [6] T. W. Haag. Design of a Thrust Stand for High Power Electric Propulsion Devices. In 25th *Joint Propulsion Conference*, Monterey, CA, 1989. AIAA-89-2829.
- [7] J.R. Anderson and D. Fitzgerald. Experimental Investigation of Fullerene Propellant for Ion Propulsion. In 23rd *International Electric Propulsion Conference*, Seattle, WA, 1993. AIAA-93-033.
- [8] J.R. Brophy, J.E. Polk, and V.K. Rawlin. Ion Engine Service Life Validation by Analysis and Testing. In 32nd *Joint Propulsion Conference*, Lake Buena Vista, FL, 1996. AIAA-96-2715.
- [9] M. Patterson, T. Haag, V. Rawlin, and M Kussmaul. NASA 30 cm Ion Thruster Development Status. In 30th *Joint Propulsion Conference*, Indianapolis, 1994. AIAA-94-2849.
- [10] V.K. Rawlin. NSTAR Memorandum: Screen Grid Wear at Low Flow and High Beam Current Conditions. Technical report, Lewis Research Center, Cleveland, OH, 1996.
- [11] J.R. Brophy. Ion Thruster Performance Model. Technical Report NASA CR- 174810, Colorado State University, Fort Collins, CO 80523, 1984.